Zeitschrift: IABSE publications = Mémoires AIPC = IVBH Abhandlungen
Band: 30 (1970)

Artikel: Failure of arches under variable repeated loading
Autor: Fukumoto, Yuhshi / Yoshida, Hiroshi
DOI: https://doi.org/10.5169/seals-23576

Failure of Arches under Variable Repeated Loading

Fissures des arcs soumis à des charges variables et répétées

Bruch von Bogen unter variabler Wechsellast

YUHSHI FUKUMOTO
Ph. D., Associate Professor of Civil Engineering, Nagoya University, Nagoya, Japan

HIROSHI YOSHIDA
M. Sc., Instructor of Civil Engineering, Kanazawa University, Kanazawa, Japan

Introduction

The reduction of the full plastic bending moment due to axial thrust on the cross section may be disregarded in plastic analysis of structures which are composed of primary bending members, such as general beams and portal frame structures.

Many papers on the ultimate load calculated by the collapse mechanism due to plastic deformation of structures and on the shakedown load such that deflection of structures stabilized under variable repeated loading were presented previously. According to them, the difference between the shakedown load and the ultimate load is not much and the ratio of these loads is less than 0.85.

The first studies on the plastic analysis of arches including the effect of axial thrust on the full plastic moment were made around 1950. Outstanding work among these is ONAT and PRAGER's study [1] introduced yield condition of a cross section for the combination of a bending moment and an axial thrust using the upper bound and the lower bound theorems is worthy of praise among them. Besides, YOKOO and YAMAGATA [2] presented an interesting paper on the collapse behaviour of arches. Numerous studies are now available on the ultimate strength of arches [3]. These include experimental studies on models.

Nevertheless, there are few studies on the shakedown load and residual deformation of arch structures under variable moving repeated load beyond elastic limit [4]. FRANCIOSI, V., AUGUSTI, G. and SARACIO, R. [5] calculated the ultimate load and the shakedown load of a reinforced concrete arch considering uniformly distributed dead load, live load and the variation of temperature.

They derived an approximation using the upper bound theorem and an iconography. According to numerical results of the computation, the shakedown load was only 38% of the ultimate load. It is much less than the ratio of the two loads calculated by considering bending moment only. Thus the axial thrust can not be ignored in the investigation of the shakedown load.

In this paper, the theoretical analysis of shakedown load of structures applying a bending moment and an axial thrust is described and the loads are calculated for two-hinged steel circular arches with "I", box or rectangular cross sections.

The calculation results are arranged and are compared for the center angles of arches, the shapes of cross sections and the depths of cross sections as parameters.

Assumptions and Yield Conditions

The assumptions in the analysis are as follows;

1. The stress-strain diagram of the material is ideally elastoplastic.
2. In the yield conditions, the bending moment and the axial thrust are considered but not the shear force.
3. There is no premature failure due to buckling or instability.

Using the above assumptions, the yield conditions are given by the following expressions, by using A_F/A_W (the ratio of both flange sectional area A_F and web sectional area A_W) and d/d_W (the ratio of the height of cross section of arch rib d and web depth d_W) as parameters, when a bending moment and an axial thrust act on a "I" or a box cross section as shown in Fig. 1.

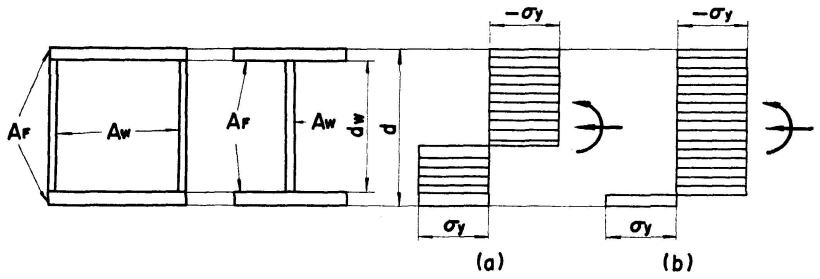

Fig. 1.

$$\left|\frac{M}{M_p}\right| = 1.0 - k\left(\frac{N}{N_y}\right)^2, \qquad 0 \leqq \frac{N}{N_y} \leqq \frac{1}{1+(A_F/A_W)}, \tag{1}$$

$$\left|\frac{M}{M_p}\right| = k'\left\{1.0 - \left(\frac{N}{N_y}\right)\right\}, \qquad \frac{1}{1+(A_F/A_W)} \leqq \frac{N}{N_y} \leqq 1.0, \tag{2}$$

where,

$$k = \frac{\{(A_F/A_W)+1.0\}^2}{\{(d/d_W)+1.0\}(A_F/A_W)+1.0},$$
$$k' = \frac{\{(d/d_W)+1.0\}\{(A_F/A_W)+1.0\}}{\{(d/d_W)+1.0\}(A_F/A_W)+1.0} \tag{3}$$

and M_p is the full plastic moment, $N_y = A\,\sigma_y$ is the yield load, $A = A_F + A_W$ is the cross sectional area, M is the bending moment, N is the axial thrust and σ_y is the yield stress. Equation (1) considers the yield condition for the bending moment and the axial thrust for the case of neutral axis in the web at the formation of plastic hinge, and Equation (2) puts yield condition for the case of neutral axis in the flange into an approximate linear expression.

Yield conditions of Eqs. (1) and (2) for the bending moment and the axial thrust for the plastic hinge formation (that is, $M/M_p = 1.0 - (N/N_y)^2$ for $A_F/A_W = 0.1$, namely for rectangular cross section and $A_F/A_W = 1.5$, 3.0 for $d/d_W = 1.1$) are illustrated in Fig. 2.

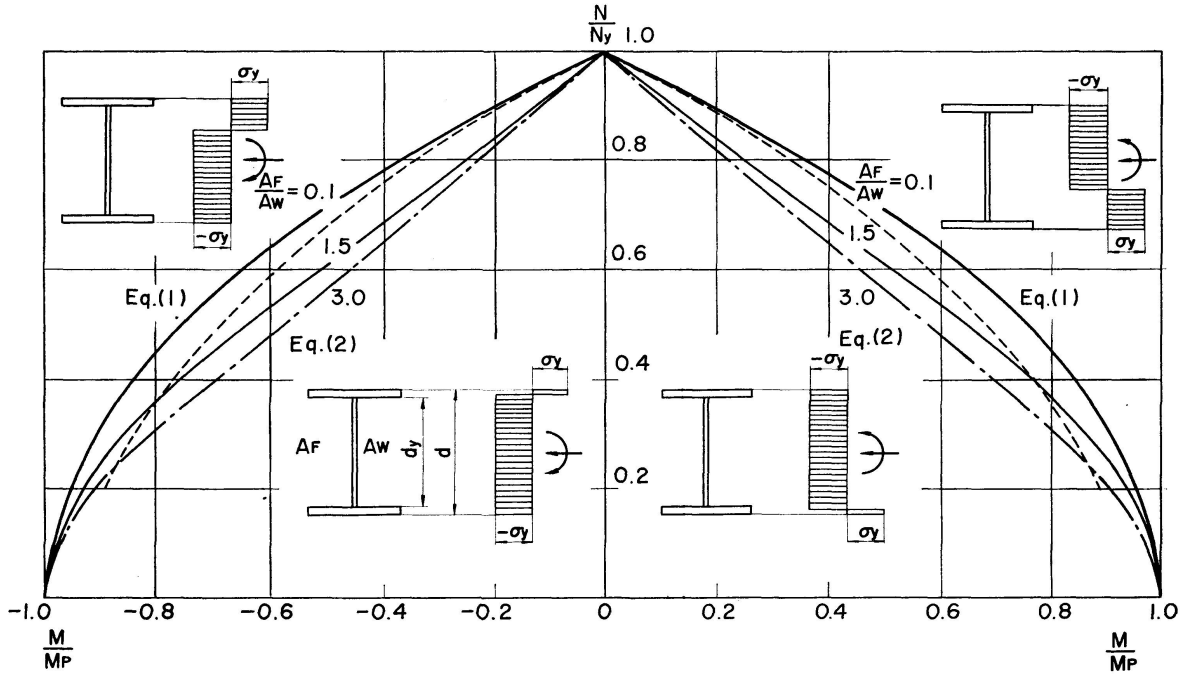

Fig. 2. Interaction Curves Between Axial Thrust and Bending Moment.

The applicable ranges for Eqs. (1) and (2) are divided by dotted line.

In the following procedures, Eqs. (1) and (2) are used as the yield conditions and A_F/A_W is used as parameter because d/d_W is approximately 1.1 in general arches with I-shaped cross sections.

Ultimate Load

The ultimate load of two-hinged circular arch having center angle 2ϕ may be calculated by lower bound theorem for the condition of uniformly distributed dead load $\alpha N_y/L_0$ per unit length and a concentrated load acting at d_0 where locates at angle θ from midspan C.

The two hinged arch under unsymmetrical load reaches collapse by the formation of two plastic hinges. If the plastic hinges form at any two cross sections, the bending moment and the axial thrust in these sections must satisfy

the yield condition of Eq. (1) or (2). However, it does not always follow that statically admissible condition is satisfied in all the cross sections, because the location of plastic hinges is assumed arbitrarily. Therefore, another assumption of locations of plastic hinges is necessary to compute the ultimate loads, and the minimum of these will give the exact ultimate load.

The procedure of analysis of the ultimate load under the loading condition shown in Fig. 3 are given as follows.

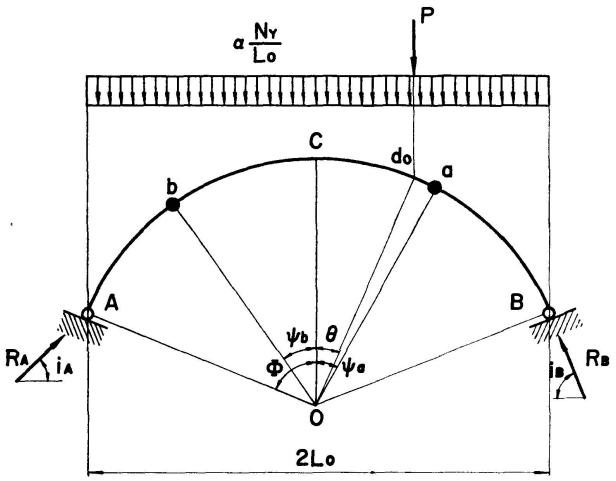

Fig. 3.

1. Let i_A be the angle between R_A, the reaction at hinged support A, and the horizontal and let i_A be unknown. The magnitude of the load P is determined from the equilibrium of hinged support B as follows.

$$P = \frac{2 \sin i_A \sin \phi}{\sin \phi - \sin \theta} R_A - \frac{2 \alpha \sin \phi}{\sin \phi - \sin \theta} N_y . \tag{4}$$

2. Assume that the plastic hinges are formed at points "a" and "b" where the angle from midspan C to support B is ψ_a and the angle from midspan C to support A is ψ_b, respectively. Let the bending moments and axial thrusts at points "a" and "b" be M_a, M_b and N_a, N_b, respectively. Consequently, the following equations are obtained.

$$\begin{aligned} M_a &= (A_a R_a + B_a N_y) L_0 , \\ N_a &= C_a R_A + D_a N_y , \end{aligned} \tag{5}$$

$$\begin{aligned} M_b &= (A_b R_a + B_b N_y) L_0 , \\ N_b &= C_b R_A + D_b N_y , \end{aligned} \tag{6}$$

where N is positive for compressive axial force and M is positive if the top flange of the cross section is in compression, and

$$\begin{aligned} A_a &= \sin i_A \operatorname{cosec} \phi (\sin \phi + \sin \psi_a) - \cos i_A \operatorname{cosec} \phi (\sin \psi_a - \cos \phi) , \\ B_a &= -\tfrac{1}{2} \alpha \operatorname{cosec}^2 \phi (\sin \phi + \sin \psi_a) , \\ C_a &= \cos i_A \operatorname{cosec} \psi_a - \sin i_A \sin \psi_a , \\ D_a &= \alpha \operatorname{cosec} \phi (\sin \phi + \sin \psi_a) \sin \psi_a , \end{aligned}$$

for $\theta \geqq \psi_a$

$$A_a = \sin i_A \operatorname{cosec}\phi\,(\sin\phi + \sin\psi_a) - \cos i_A \operatorname{cosec}\phi\,(\cos\psi_a - \cos\phi)$$
$$- 2\operatorname{cosec}\phi\,(\sin\psi_a - \sin\theta)\sin i_A \sin\phi/(\sin\phi - \sin\theta),$$
$$B_a = -\tfrac{1}{2}\alpha \operatorname{cosec}^2\phi\,(\sin\phi + \sin\psi_a)^2 + 2\operatorname{cosec}\phi\,(\sin\psi_a - \sin\theta)\,\alpha\sin\phi/(\sin\phi - \sin\theta),$$
$$C_a = \cos i_A \cos\psi_a - \sin i_A \sin\psi_a + 2\sin i_A \sin\theta/(\sin\phi - \sin\theta)\cdot\sin\psi_a,$$
$$D_a = \alpha\operatorname{cosec}\phi\,(\sin\phi + \sin\psi_a)\sin\psi_a - 2\,\alpha\sin\phi/(\sin\phi - \sin\theta)\cdot\sin\psi_a,$$

for $\theta \leqq \psi_a$

$$A_b = \sin i_A \operatorname{cosec}\phi\,(\sin\phi - \sin\psi_a) - \cos i_A \operatorname{cosec}\phi\,(\cos\psi_b - \cos\phi),$$
$$B_b = -\tfrac{1}{2}\alpha \operatorname{cosec}^2\phi\,(\sin\phi - \sin\psi_b)^2,$$
$$C_b = \cos i_A \cos\psi_b + \sin i_A \sin\psi_b,$$
$$D_b = -\alpha\operatorname{cosec}\phi\,(\sin\phi - \sin\psi_b)\sin\psi_b.$$

3. The yield condition must satisfy Eq. (1) or (2), according as the axial thrusts are smaller or larger than $1/(1 + A_F/A_W)$, respectively. On the other hand, the magnitudes of these axial thrusts are decided by the locations of the concentrated load. As shown in Fig. 3, the axial thrust at point "b" is always larger than that at point "a" when the location of P is nearer to support B from the center of the span. Therefore, three cases are possible as to the location of the neutral axis of the cross section. That is,

a) neutral axes in web at points "a" and "b",

b) neutral axes in web at point "a" and in flange at point "b",

c) both neutral axes in flange at points "a" and "b".

The yield condition, Eq. (1) or (2) has to be satisfied by substituting Eqs. (5) and (6) at points "a" and "b" depending on the location of the neutral axis.

4. It can be known from the condition $N/N_y \gtrless 1/\{1 + (A_F/A_W)\}$ using N obtained in items a), b) and c) whether the assumed locations of neutral axes in cross sections are correct or not, where N is the actual thrust at point "a" or "b" calculated from item a), b) or c).

5. P is determined by substituting Eq. (4) to valid R_A and i_A determined hitherto.

6. Ultimate load P is derived under the assumption that the plastic hinges form at the arbitrarily assumed points "a" and "b". But it does not always follow that a atatically admissible condition is obtained. To obtain a statically admissible condition, the minimum value of P must be determined for all the combinations of ψ_a and ψ_b. Then, the minimum value of P is the ultimate load under the given load location.

7. The ultimate load P is given as the minimum value of P derived by

repeating the above mentioned sequences (1) to (6) under varying load location of 0 to ϕ.

The numerical results of the above analysis are summarized at the end of this paper.

Shakedown Load

Shakedown loading is shown in Fig. 4. When a concentrated load, $P=0.1442\ N_y$ moves in the arch having the center angle $2\phi=120°$ as shown in Fig. 4(a) and the arch rib of which cross section has $d/d_w=1.1$ and $A_F/A_W=1.5$. The influence lines of elastic bending moment and axial force due to $P=0.1442\ N_y$ at points "a" and "b" are shown by the curves 1 and 3 in Fig. 4(a) and (b),

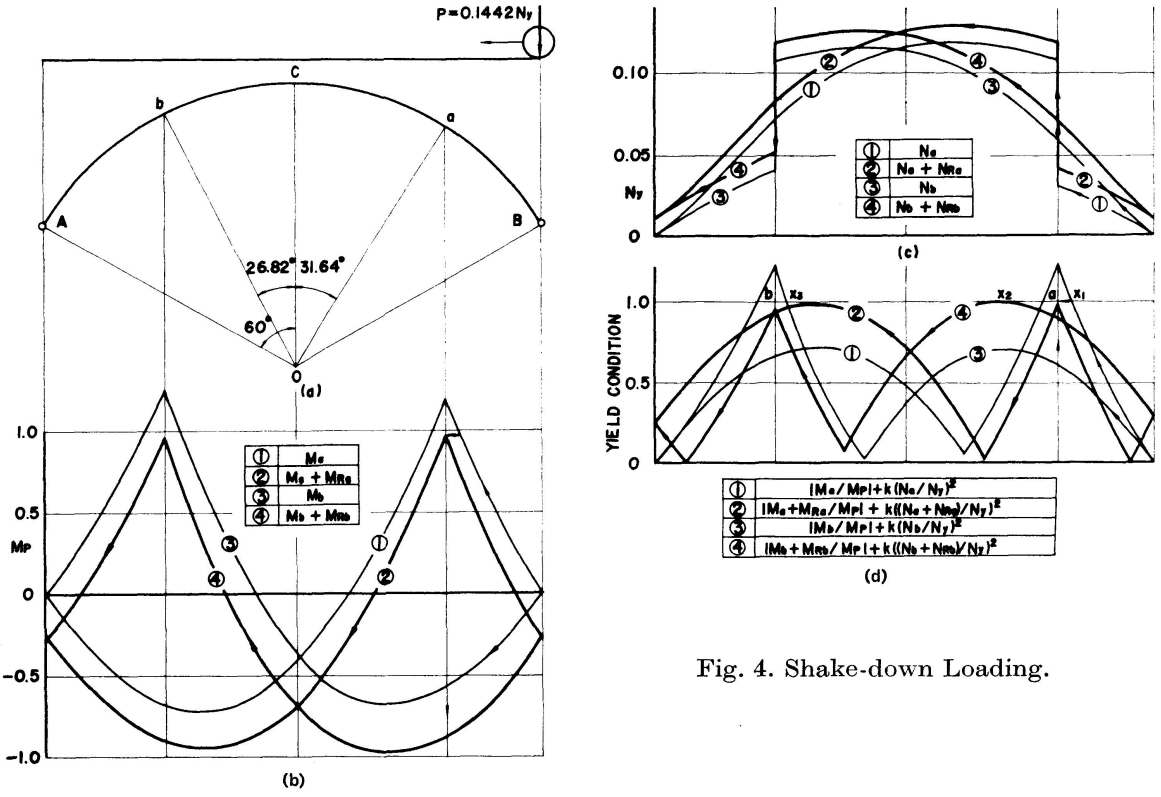

Fig. 4. Shake-down Loading.

respectively, where M_{ax}, M_{bx} and N_{ax}, N_{bx} are the bending moments and the axial thrusts at points "a" and "b", respectively and the bending moment and the axial thrust in Figs. 4(b) and (c) are nondimensionalized by M_p and N_y, respectively. The values of the right term of the yield condition, $|M_{ax}/M_p| + k(N_{ax}/N_y)^2$ and $|M_{bx}/M_p| + k(N_{bx}/N_y)^2$ are indicated by the cuves 1 and 3 in Fig. 4(d). When at first the load is at support B, M_{ax} and N_{ax} are zero. As the load moves further, M_{ax} and N_{ax} increase and when the load reaches point x_1, $|M_{ax}/M_p| + k(N_{ax}/N_y)^2$ attains a value of 1.0. After the load passes x_1, the rotation of plastic hinge at "a" begins. When the load passes point "a", the rotation of plastic hinge at "a" becomes the maximum. Even if the load is

removed at this point, there are residual bending moment and axial thrust due to plastic deformation.

Therefore, as the load passes through the point "a", residual bending moment M_{ra} and residual axial thrust N_{ra} in addition to elastic bending moment M_{ax} and elastic axial thrust N_{ax} appear at point "a". The curves 2 and 4 in Figs. 4(b) and (c) show respectively the influence lines of bending moments and those of axial thrusts at points "a" and "b" considering the effects of residual bending moments and axial thrusts. And the combination of them, $|(M_{ax}+M_{ra})/M_p|+k(N_{bx}+N_{rb})/N_y)^2$, is shown by the curve 2 in Fig. 4(d). This value never exceed 1.0 hereafter. On the other hand, the bending moment and the axial thrust at point "b" are zero when the load is at the support B, the absolute values of M_{bx} and N_{bx} and their combination, $|M_{bx}/M_p|+k(N_{bx}/N_y)$ also increase with moving of the load. When the load reaches point "a", residual bending moment M_{br} and residual thrust N_{br} due to the plastic deformation at point "a" appear at point "b" in addition to elastic bending moment M_{bx} and elastic axial thrust N_{bx}. As the load passes through this point "a", their combination becomes $|(M_{bx}+M_{rb})/M_p|+k[(N_{bx}+N_{rb})/N_y]^2$ and this value becomes 1.0 when the load passes point x_2, and a plastic hinge is formed at point "b". But after the load passes this point x_2, the value decreases immediately and the plastic deformation at point "b" does not remain. If the load is slightly greater than $P=0.1442P_y$ the plastic deformation would yield at point "b". With further moving of the load, $|(M_{bx}+M_{rb})/M_p|+k[(N_{bx}+N_{rb})/N_y]^2$ decreases. It increases again along curve 3, and when the load passes through point "x_3", $|(M_{ax}+M_{ra})/M_p|+k([N_{bx}+N_{rb})/N_y]^2$ becomes 1.0 and it would exceed 1.0 at point "b". However, according to the residual deformation at point "a", the combination of bending moment and axial thrust $|(M_{bx}+M_{ra})/M_p|+k[(N_{bx}+N_{rb})/N_y]^2$ is less than 1.0 as shown by curve 4 in Fig. 4(d). Therefore, a plastic hinge does not form at point "b". For the first cycle of loading, the variation of the bending moment, the axial

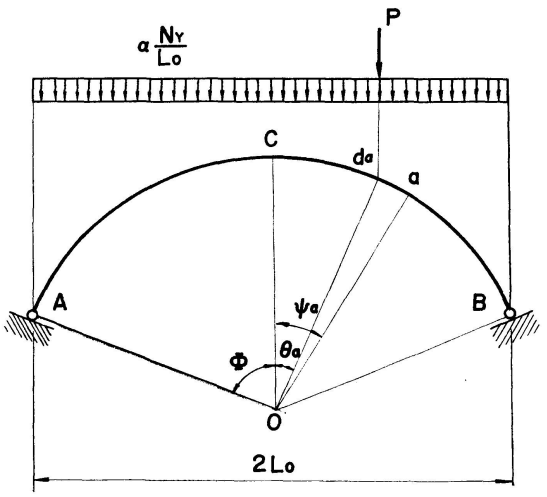

Fig. 5.

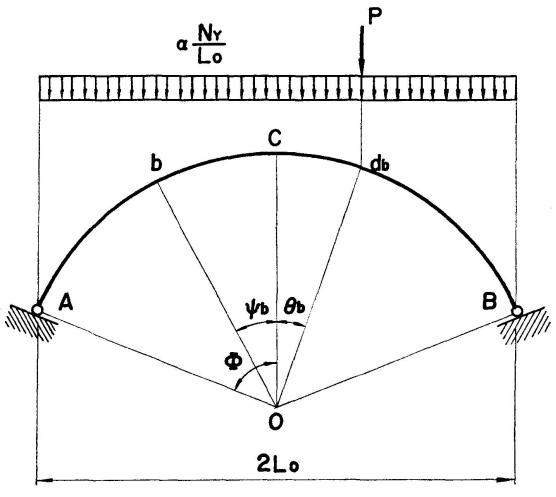

Fig. 6.

thrust and their combination follow the direction of the arrow as shown in Figs. 4(b), (c) and (d). After the second cycle of the moving load, their variations follow along the heavy line as shown by curves 2 and 4 in Figs. 4(b), (c) and (d) and the plastic hinges form instantaneously but plastic deformation does not increase. Thus, after the second cycle of loading, the arch behaves elastically under the moving load $P=0.1442\,N_y$. This is called shakedown and the corresponding load $P=0.1442\,N_y$ is a shakedown load.

The method of obtaining the shakedown load by lower bound theory will be described below.

Let the elastic bending moment and the elastic axial thrust at point "a" under a concentrated load and uniformly distributed load as shown in Fig. 5 be M_a and N_a, respectively.

$$\begin{aligned} M_a &= (A_{Ma}\,P + B_{Ma}\,N_y)\,L_0\,, \\ N_a &= A_{Na}\,P + B_{Na}\,N_y\,. \end{aligned} \tag{7}$$

Also, let the elastic bending moment and the elastic axial thrust at point "b" under the loading condition as shown in Fig. 6 be M_b and N_b, respectively,

$$\begin{aligned} M_b &= (A_{Mb}\,P + B_{Mb}\,N_y)\,L_0\,, \\ N_b &= A_{Nb}\,P + B_{Nb}\,N_y\,, \end{aligned} \tag{8}$$

where,

$$\begin{aligned} A_{Ma} &= (\sin\phi - \sin\theta_a)/2\sin\phi\cdot\operatorname{cosec}\phi\,(\sin\phi+\sin\psi_a) - A_a\operatorname{cosec}\phi\,(\cos\psi_a-\cos\phi)\,, \\ B_{Ma} &= \alpha\operatorname{cosec}\phi\,(\sin\phi+\sin\psi_a) - B_a\operatorname{cosec}\phi)\,(\cos\psi_a-\cos\phi) \\ &\quad -\tfrac{1}{2}\alpha\operatorname{cosec}^2\phi\,(\sin\phi+\sin\psi_a)^2\,, \\ A_{Na} &= A_a\cos\psi_a - (\sin\phi-\sin\theta_a)/2\sin\phi_a\cdot\sin\psi_a\,, \\ B_{Na} &= B_a\cos\psi_a - (\sin\phi+\sin\theta_a)/2\sin\phi\sin\psi_a + \alpha\operatorname{cosec}\phi\,(\sin\phi+\sin\psi_a)\sin\psi_a\,, \\ &\qquad \psi_a \leqq \theta_a\,. \end{aligned}$$

$$\begin{aligned} A_{Ma} &= (\sin\phi+\sin\theta_a)/2\sin\phi\cdot\operatorname{cosec}\phi\,(\sin\phi-\sin\psi_a) - A_a\operatorname{cosec}\phi\,(\cos\psi_a-\cos\phi)\,, \\ B_{Ma} &= \alpha\operatorname{cosec}\phi\,(\sin\phi-\sin\psi_a) - B_a\operatorname{cosec}\phi\,(\cos\psi_a-\cos\phi) \\ &\quad -\tfrac{1}{2}\alpha\operatorname{cosec}^2\phi\,(\sin\phi-\sin\psi_a)^2\,, \\ A_{Na} &= A_a\cos\psi_a + (\sin\phi+\sin\theta_a)/2\sin\phi\cdot\sin\psi_a\,, \\ B_{Na} &= B_a\cos\psi_a + \alpha\sin\psi_a - \alpha\operatorname{cosec}\phi\sin\psi_a\,(\sin\phi-\sin\psi_a)\,, \\ &\qquad \psi_a \geqq \theta_a\,. \end{aligned}$$

$$\begin{aligned} A_{Mb} &= (\sin\phi-\sin\theta_b)/2\sin\phi\cdot\operatorname{cosec}\phi\,(\sin\phi-\sin\psi_b) - A_b\operatorname{cosec}\phi\,(\cos\psi_b-\cos\phi)\,, \\ B_{Mb} &= \alpha\operatorname{cosec}\phi\,(\sin\phi-\sin\psi_b) - B_a\operatorname{cosec}\phi\,(\cos\psi_b-\cos\phi) \\ &\quad -\tfrac{1}{2}\alpha\operatorname{cosec}^2\phi\,(\sin\phi-\sin\psi_b)^2\,, \\ A_{Nb} &= A_b\cos\psi_b + (\sin\phi-\sin\theta_b)/2\sin\phi\cdot\sin\psi_b\,, \end{aligned}$$

$$
\begin{aligned}
B_{Nb} &= B_a \cos\psi_b + \alpha \sin\psi_b - \alpha \operatorname{cosec}\phi \sin\psi_b (\sin\phi - \sin\psi_b),\\
A_a &= \tfrac{1}{2}[\sin^2\phi - \sin^2\theta_a - 2\cos\phi(\phi\sin\phi - \theta_a\sin\theta_a + \cos\phi - \cos\theta_a)\\
&\quad - \gamma(\sin^2\phi - \sin^2\theta_a)]/[\phi - 3\sin\phi\cos\phi + 2\phi\cos^2\phi + \gamma(\phi + \sin\phi\cos\phi)],\\
B_a &= \frac{\alpha}{2}[4/3\cdot\sin^3\phi + \phi\cos\phi - 2\phi\sin^2\phi\cos\phi - \sin\phi\cos^2\phi + 2\gamma(\phi\cos^2\phi - \tfrac{1}{2}\phi\\
&\quad - \tfrac{1}{2}\sin\phi\cos\phi)]/[\phi - 3\sin\phi\cos\phi + 2\phi\cos^2\phi + \gamma(\phi + \sin\phi\cos\phi)],\\
A_b &= \tfrac{1}{2}[\sin^2\phi - \sin^2\theta_b - 2\cos\phi(\phi\sin\phi - \theta_b\sin\theta_b + \cos\phi - \cos\theta_b)\\
&\quad - \gamma(\sin^2\phi - \sin^2\theta_b)]/[\phi - 3\sin\phi\cos\phi + 2\phi\cos^2\phi + \gamma(\phi + \sin\phi\cos\phi)],\\
\gamma &= \frac{12\{1 + (A_F/A_W)\}}{3[1 + \frac{1}{2}\{(d/d_w) - 1\}^2(A_F/A_W) + 1}\,\frac{1}{\delta(d/d_w)^2},\\
\delta &= d/L_0.
\end{aligned}
\tag{9}
$$

On the other hand, the residual reaction due to the residual deformation are only a horizontal reaction H_R as shown in Fig. 7. Then the residual bending

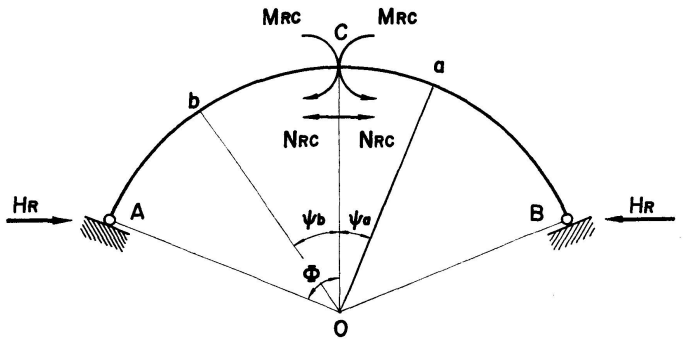

Fig. 7.

moments M_{Ra}, M_{Rb} and residual axial thrusts N_{Ra}, N_{Rb} at points "a" and "b" are given by

$$
\begin{aligned}
M_{Ra} &= -\operatorname{cosec}\phi(\cos\psi_a - \cos\phi) H_R L_0,\\
N_{Ra} &= H_R \cos\psi_a,
\end{aligned}
\tag{10}
$$

$$
\begin{aligned}
M_{Rb} &= -\operatorname{cosec}\phi(\cos\psi_b - \cos\phi) H_R L_0,\\
N_{Rb} &= H_R \cos\psi_b.
\end{aligned}
\tag{11}
$$

Now, if plastic hinges are formed at points "a" and "b", the sum of the elastic bending moment and the residual bending moment and the sum of the elastic axial thrust and the residual axial thrust at points "a" and "b", respectively, must satisfy the yield condition of Eq. (1) or (2).

When P is on the right half of the span, the axial thrust at point "b" is always larger than that at point "a". Therefore, the location of neutral axis of cross section at the yield hinge formation is divided into three cases.

a) Neutral axes in web at points "a" and "b"

The yield condition Eq. (1) must be satisfied at points "*a*" and "*b*", respectively. Therefore, applying Eqs. (7), (10) and Eqs. (8), (11) to Eq. (1), respectively, the following expressions are obtained.

$$\begin{aligned}\frac{(A_{Ma}P+B_{Ma}N_y)L_0+M_{Ra}}{M_p}-k\left(\frac{A_{Na}P+B_{Na}N_y+N_{Ra}}{N_y}\right)^2&=1.00,\\ \frac{(A_{Mb}P+B_{Mb}N_y)L_0+M_{Rb}}{M_p}-k\left(\frac{A_{Nb}P+B_{Nb}N_y+N_{Rb}}{N_y}\right)^2&=1.00.\end{aligned}\tag{12}$$

Using the following symbols;

$$\frac{P}{N_y}=Q,\quad \frac{H_R}{N_y}=R,\quad \frac{M_p}{N_y}=\frac{Z}{A}=\lambda d,\quad \lambda=\frac{(A_F/A_W)+1}{4k(d/d_w)}.\tag{13}$$

Eq. (12) can be rewritten as,

$$\begin{aligned}a_1Q+b_1R+c_1&=1.00-k(A_{Na}Q+R\cos\psi_a+B_{Na})^2,\\ a_2Q+b_2R+c_2&=1.00-k(A_{Nb}Q+R\cos\psi_b+B_{Nb})^2,\end{aligned}\tag{14}$$

where,

$$\begin{aligned}a_1&=A_{Ma}/\lambda\delta, & b_1&=\operatorname{cosec}\phi(\cos\psi_a-\cos\phi)/\lambda\delta,\\ a_2&=-A_{Mb}/\lambda\delta, & b_2&=\operatorname{cosec}\phi(\cos\psi_b-\cos\phi)/\lambda\delta,\\ c_1&=B_{Ma}/\lambda\delta, & c_2&=-B_{Mb}/\lambda\delta.\end{aligned}\tag{15}$$

Q and R can be determined from Eqs. (14).

b) Neutral axes in web at point "a" and in flange at point "b"

The yield condition Eq. (1) and (2) must be satisfied at points "*a*" and "*b*", respectively. Therefore, by substituting Eqs. (7) and (10) into Eq. (1), and Eqs. (8) and (10) to Eq. (2) and combining with Eqs. (13) and (15);

$$\begin{aligned}a_1Q+b_1R+c_1&=1.00-k(A_{Na}Q+R\cos\psi_a+B_{Na}),\\ a_2Q+b_2R+c_2&=k'\{1.00-(A_{Nb}Q+R\cos\psi_a+B_{Nb})\}\end{aligned}\tag{16}$$

are obtained. Q and R can be determined from Eqs. (16).

c) Both neutral axes in flange at points "a" and "b"

The yield condition Eq. (2) must be satisfied at both points "*a*" and "*b*". By substituting Eqs. (7), (16) and Eqs. (15), (11) into Eq. (2), respectively and using Eqs. (13) and (15);

$$\begin{aligned}a_1Q+b_1R+c_1&=k'\{1.00-(A_{Na}Q+R\cos\psi_a+B_{Na})\},\\ a_2Q+b_2R+c_2&=k'\{1.00-(A_{Nb}Q+R\cos\psi_b+B_{Nb})\}\end{aligned}\tag{17}$$

are obtained. Q and R can be determined from Eqs. (17).

Locations of the neutral axes of cross-sections "a" and "b" at plastic hinges are in the web or in the flange can be found from the conditions of $N/N_y \lesseqgtr 1/(1+A_F/A_W)$ where N's are the actual thrusts at points "a" and "b" and they are calculated from Q and R determined in a) to c), respectively. If they coincide with the assumed ones, Q and R become the true values. P is thus determined from the valid Q and R using Eq. (13).

Above is the shakedown load obtained under an assumption that a plastic hinge is formed at point "a" under the combination of uniformly distributed load and a concentrated load at point d_a as shown in Fig. 5 and the other plastic hinge is formed at point "b" under the combination of uniformly distributed load and a concentrated load at point "d_b". However, it does not always follow that the statically admissible condition is fulfilled. In order that it is always, the minimum value of P must be determined for every combination of ψ_a and ψ_b.

Hitherto, it is considered that the concentrated load is located at the points rotated by angle θ_a and θ_b from midspan C to support B, respectively. Since a concentrated load could be applied at any arbitrary points, the shakedown load, which is taken into account of moving of a concentrated load is the minimum value for every combination of θ_a and θ_b varying from $-\phi$ to ϕ, respectively.

The numerical results are summarized at the end of this paper.

Alternating Plasticity Load

When a cross section is subjected to alternating plasticity, fracture may occur after a few hundred applications of loads. If the maximum fiber stress at a point on a cross section under a loading condition is σ_{max} and the minimum

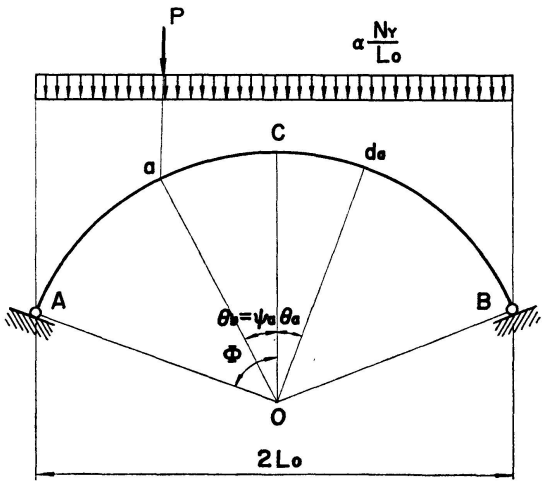

Fig. 8.

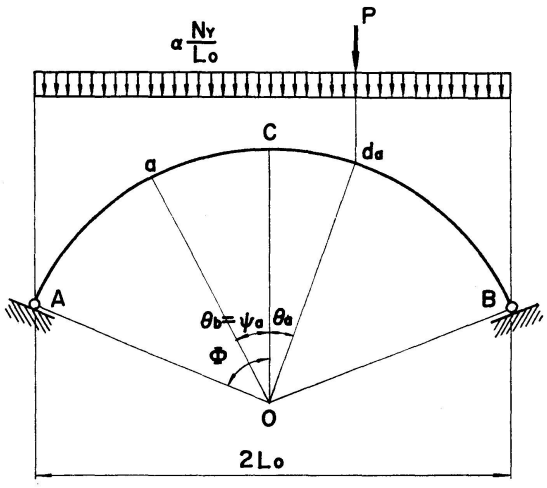

Fig. 9.

fiber stress at the same point under the load condition is σ_{min}, alternating plasticity failure occurs at such a section if the following condition is satisfied.

$$\sigma_{max} - \sigma_{min} \geqq 2\sigma_y. \tag{18}$$

Let the positive bending moment at point "a" under a loading condition as shown in Fig. 8 be M_1 and the negative bending moment at point "a" under a loading condition as shown in Fig. 9 be M_2, and let the axial thrusts under those conditions be N_1 and N_2, respectively, then by applying the positive and negative fiber stress on the section "a" to Eq. (18)

$$\begin{aligned} &\left| (M_1 - M_2)\frac{A\,d}{2\,I} - (N_1 - N_2) \right| \geqq 2\,N_y, \\ &\left| -(M_1 - M_2)\frac{A\,d}{2\,I} - (N_1 - N_2) \right| \geqq 2\,N_y \end{aligned} \tag{19}$$

are obtained, where I is the moment of inertia of the cross section.

Introducing M_1, M_2, N_1 and N_2 into Eqs. (7) and (8), the terms referring to the uniformly distributed load vanish and Eq. (19) can be arranged as follows:

$$\begin{aligned} &\left| (A_{Ma} - A_{Mb})\,\eta - (A_{Na} - A_{Nb}) \right| P \geqq 2\,N_y, \\ &\left| -(A_{Ma} - A_{Mb})\,\eta - (A_{Na} - A_{Nb}) \right| P \geqq 2\,N_y, \end{aligned} \tag{20}$$

where,

$$\eta = \frac{2\{(A_F/A_W) + 1\}(d/d_w)^2}{([1 + \frac{1}{2}\{(d/d_w) - 1\}]^2 (A_F/A_W) + \frac{1}{3})\,\delta}.$$

The smaller value of P determined from Eqs. (20) is the alternating plasticity failure occurs at point "a".

As point "a" is assumed arbitrarily, the minimum value of P under variation of ψ_a from zero to ϕ is the alternating plasticity load under the assumption that the loading conditions as shown in Figs. 8 and 9 act alternatingly.

Now, this alternating plasticity load was obtained under the loading condition that a concentrated load is located at point "a" with angle θ_a from midspan C to support A and at point with angle θ_b to support B. Since a concentrated load may be located arbitrarily, the alternating plasticity load, considering any combinations of θ_a and θ_b varying from zero to ϕ, respectively.

The numerical results on alternating load are summarized at the end of this paper.

Numerical Results and Discussions

The numerical results of the ultimate load, shakedown load and alternating plasticity load calculated by the above mentioned methods are shown below and the comparisons are made among them. The parameters used for the computation are $d/L_0 = 0.02$, 0.05 and 0.10, $d/d_W = 1.1$ and $A_F/A_W = 0.1$, 1.5 and 3.0, where d is the height of arch rib section, L_0 half length of span, d_W the depth of web of arch rib, A_F the total sectional area of both flanges and A_W

is sectional area of the web. The half center angle of arches ϕ varies from 10 degrees to 90 degrees and the pitch is 10 degrees. As on general arch sections d/d_W is considered to be in the range 1.10 to 1.14, 1.1 is used as d/d_W hereupon. $A_F/A_W = 0.1$ indicates a rectangular cross section when d/d_W is 1.1. And as on general arch sections the range of A_F/A_W is considered to be in the range from 1.0 to 3.0, 1.5 and 3.0 are used as A_F/A_W. As for uniformly distributed loads ($w = \alpha N_y/L_0$), 0.02, 0.05 and 0.10 are used as α for $d/L_0 =$ 0.02, 0.05 and 0.10, respectively.

1. Ultimate Load

a) Ultimate load. The ultimate load due to a concentrated, uniform and combined loadings are shown in Figs. 10, 11 and 12, respectively. The values are nondimensionalized by $N_y (= A\sigma_y)$. The numerical results neglecting axial thrusts are also shown by dotted lines in the figures. As these figures show, the effect of axial thrust is small for $\phi = 80°$ to $90°$ and is particularly insignificance when d/L_0 and A_F/A_W are small.

But when ϕ is small, particularly when d/L_0 and A_F/A_W are large, its effect cannot be disregarded. Particularly, for an ultimate load due to the uniformly distributed or combined load, the effect becomes predominant. These figures show only for the case where neutral axes at plastic hinges are in web.

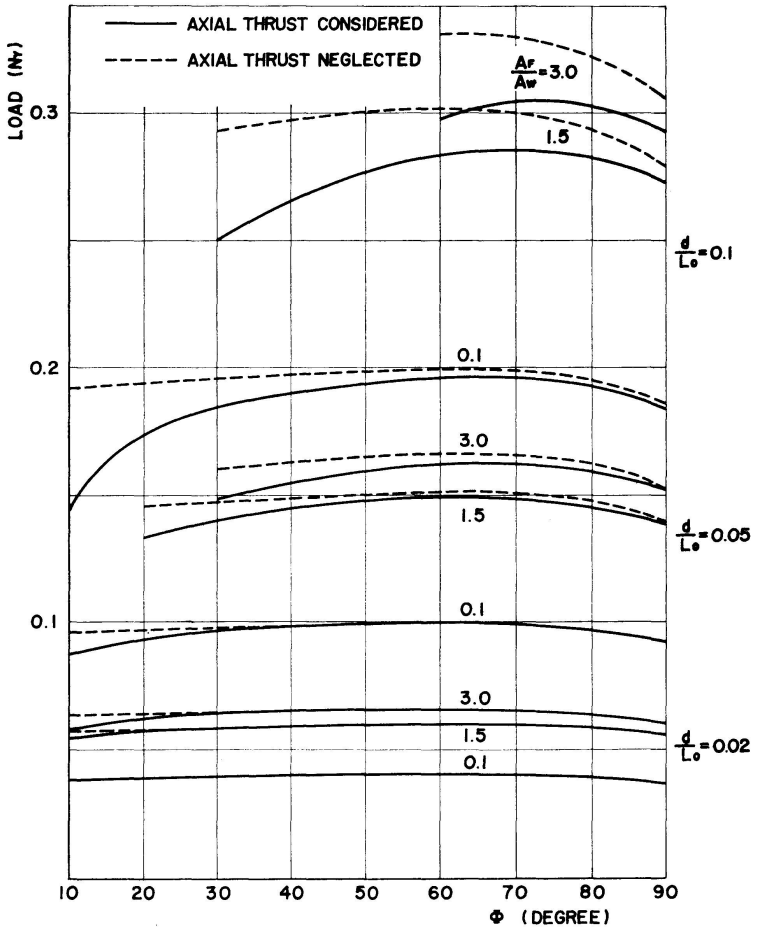

Fig. 10. Ultimate Load (Concentrated Loading).

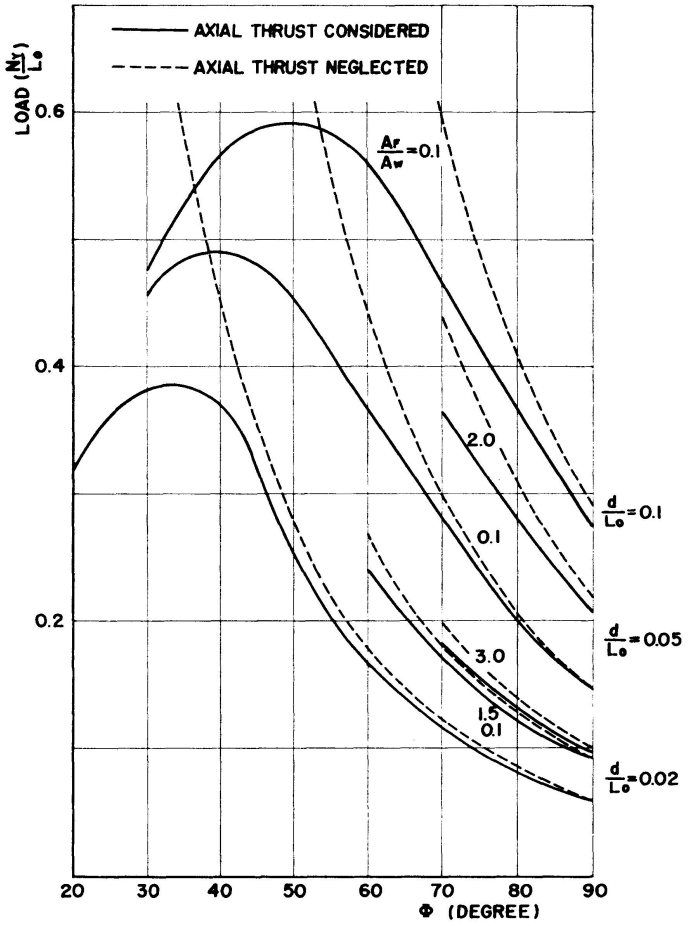

Fig. 11. Ultimate Load (Uniform Loading).

Table 1. Ultimate Load and Shake-down Load (Concentrated Loading)

(N_y)

d/L_0	A_F/A_W	ϕ								
		10°	20°	30°	40°	50°	60°	70°	80°	90°
0.02	0.1	0.0378*	0.0385	0.0388	0.0392	0.0396	0.0399	0.0399	0.0399	0.0371
		0.0363**	0.0369	0.0373	0.0378	0.0383	0.0389	0.0392	0.0389	0.0369
	1.5	0.0548	0.0574	0.0583	0.0590	0.0597	0.0602	0.0600	0.0588	0.0559
		0.0528	0.0551	0.0560	0.0568	0.0576	0.0585	0.0591	0.0586	0.0557
	3.0	0.0579	0.0624	0.0637	0.0646	0.0654	0.0660	0.0659	0.0646	0.0614
		0.0558	0.0599	0.0612	0.0622	0.0632	0.0642	0.0648	0.0643	0.0612
0.05	0.1	—	0.1269	0.1324	0.1353	0.1375	0.1390	0.1391	0.1365	0.1299
		0.0844	0.0903	0.0922	0.0937	0.0952	0.0967	0.0977	0.0970	0.0922
	1.5	—	0.1330	0.1402	0.1439	0.1465	0.1483	0.1485	0.1458	0.1388
		0.1073	0.1284	0.1349	0.1386	0.1415	0.1442	0.1460	0.1452	0.1386
	3.0	—	—	0.1492	0.1548	0.1586	0.1610	0.1616	0.1591	0.1518
		—	—	0.1436	0.1491	0.1531	0.1564	0.1588	0.1583	0.1516
0.10	0.1	0.1413	0.1739	0.1844	0.1898	0.1935	0.1960	0.1963	0.1929	0.1838
		0.1386	0.1688	0.1779	0.1830	0.1870	0.1906	0.1930	0.1921	0.1835
	1.5	—	—	0.2494	0.2659	0.2762	0.2830	0.2861	0.2834	0.2720
		—	0.2134	0.2419	0.2569	0.2669	0.2748	0.2804	0.2815	0.2719
	3.0	—	—	—	—	—	0.2982	0.3039	0.3033	0.2931
		—	—	—	0.2641	0.2784	0.2889	0.2969	0.3003	0.2931

* Upper Lines indicate for Ultimate Laod ** Lower Lines indicate for Shake-down Load

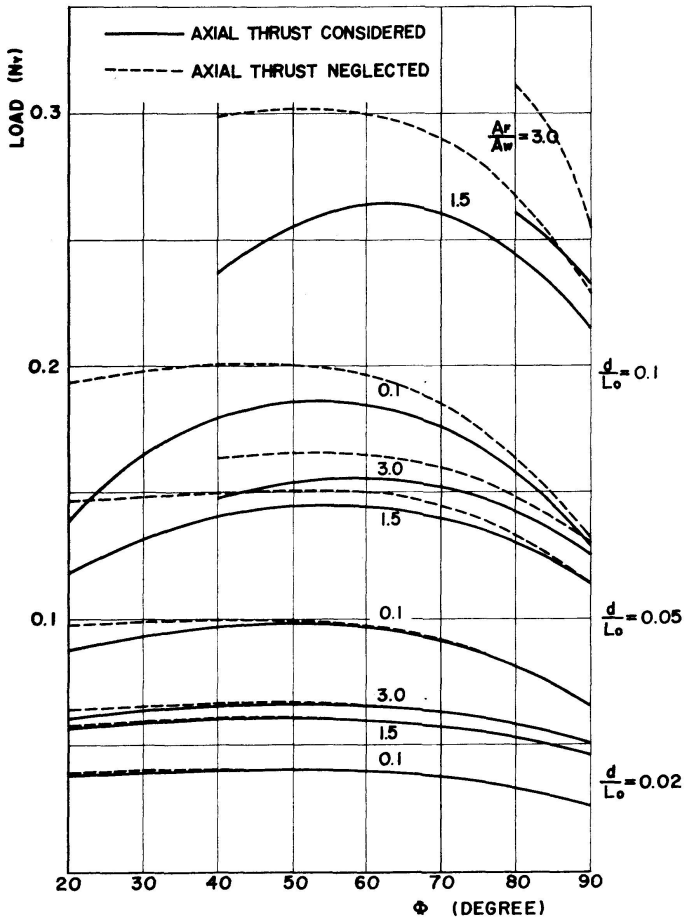

Fig. 12. Ultimate Load (Combined Loading).

Table 2. Ultimate Load and Shake-down Load (Combined Loading)
(N_y)

d/L_0	α	A_F/A_W	ϕ							
			20°	30°	40°	50°	60°	70°	80°	90°
0.02	0.02	0.1	0.0382*	0.0390	0.0396	0.0399	0.0392	0.0371	0.0329	0.0265
			0.0378**	0.0376	0.0383	0.0388	0.0388	0.0371	0.0323	0.0260
		1.5	0.0563	0.0581	0.0592	0.0599	0.0597	0.0577	0.0533	0.0460
			—	0.0562	0.0571	0.0581	0.0586	0.0576	0.0528	0.0453
		3.0	0.0604	0.0631	0.0646	0.0655	0.0654	0.0636	0.0591	0.0516
			—	0.0610	0.0623	0.0635	0.0642	0.0634	0.0587	0.0508
0.05	0.05	0.1	0.0883	0.0939	0.0968	0.0981	0.0969	0.0918	0.0815	0.0659
			—	0.0919	0.0938	0.0956	0.0959	0.0918	0.0801	0.0647
		1.5	0.1179	0.1327	0.1399	0.1439	0.1448	0.1410	0.1306	0.1133
			—	0.1313	0.1357	0.1397	0.1422	0.1406	0.1299	0.1118
		3.0	—	—	0.1476	0.1536	0.1559	0.1531	0.1435	0.1260
			—	—	0.1432	0.1490	0.1527	0.1523	0.1430	0.1245
0.10	0.10	0.1	0.1375	0.1654	0.1788	0.1856	0.1859	0.1776	0.1586	0.1287
			—	0.1654	0.1747	0.1811	0.1837	0.1776	0.1564	0.1267
		1.5	—	—	0.2353	0.2537	0.2628	0.2613	0.2460	0.2155
			—	—	0.2313	0.2468	0.2573	0.2597	0.2455	0.2137
		3.0	—	—	—	—	—	—	0.2608	0.2328
			—	—	—	—	—	—	0.2608	0.2318

* Upper Lines indicate for Ultimate Load ** Lower Lines indicate for Shake-down Load

Numerical results are summarized in Tables 1 and 2 together with the shake-down load.

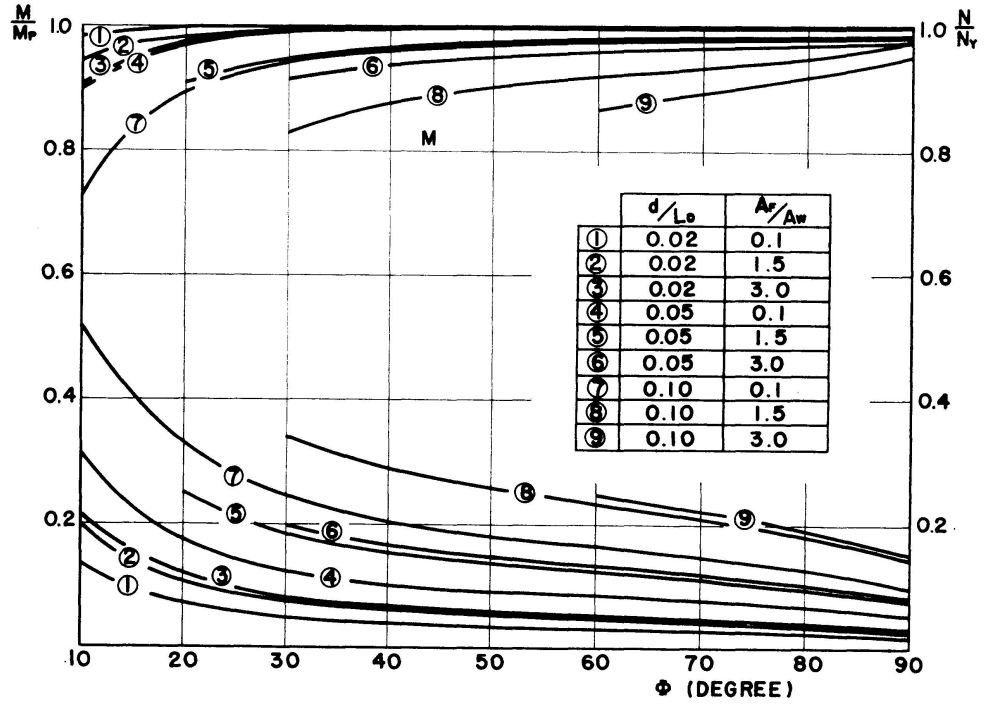

Fig. 13. Critical Bending Moment and Axial Thrust at Hinge "*a*" Under Concentrated Loading.

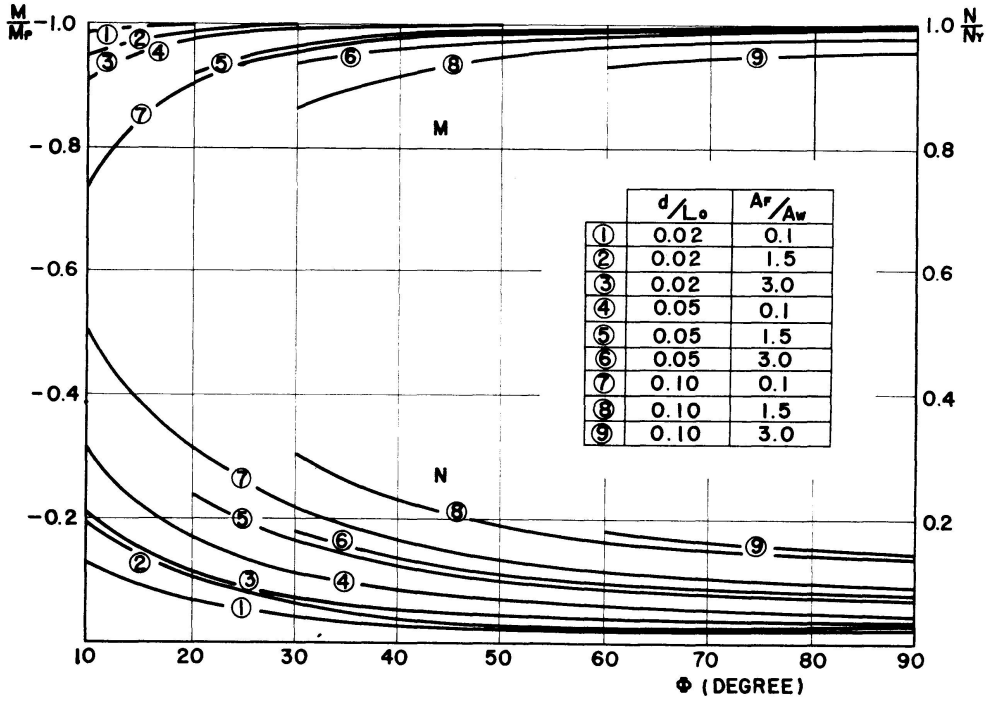

Fig. 14. Critical Bending Moment and Axial Thrust at Hinge "*b*" Under Concentrated Loading.

b) Bending moment and axial thrust at a plastic hinge. The magnitudes of bending moments and axial thrusts at plastic hinges "*a*" and "*b*" at the collapse of arches due to a concentrated and combined loadings are shown in Figs. 13, 14, 15 and 16, respectively. From these figures also, it is clear that axial thrusts increase and bending moments descrease as ϕ descreases. This tendency is remarkable for uniformly distributed load.

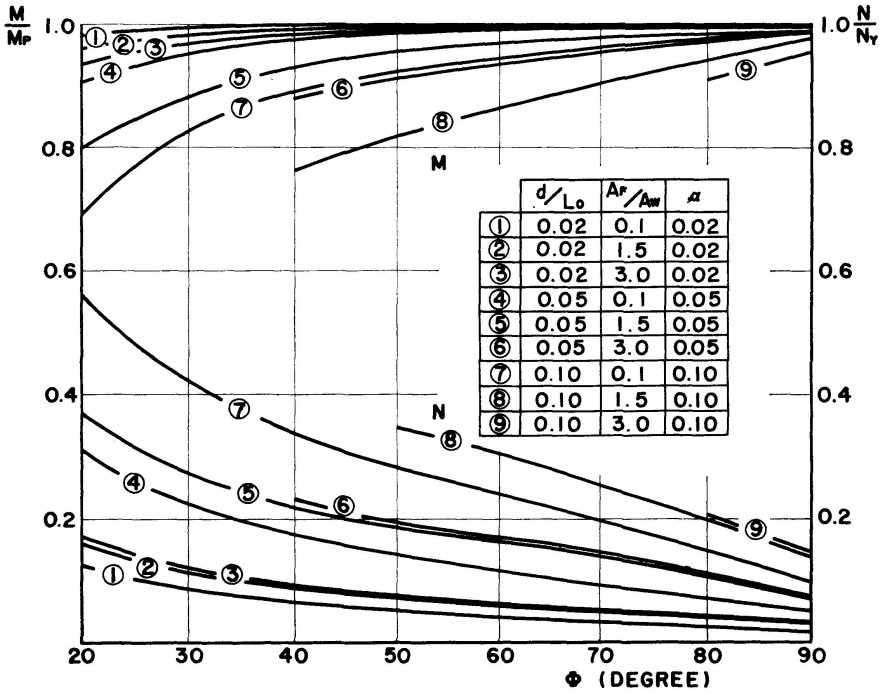

	d/L₀	Af/Aw	α
①	0.02	0.1	0.02
②	0.02	1.5	0.02
③	0.02	3.0	0.02
④	0.05	0.1	0.05
⑤	0.05	1.5	0.05
⑥	0.05	3.0	0.05
⑦	0.10	0.1	0.10
⑧	0.10	1.5	0.10
⑨	0.10	3.0	0.10

Fig. 15. Critical Bending Moment and Axial Thrust at Hinge "*a*" Under Combined Loading.

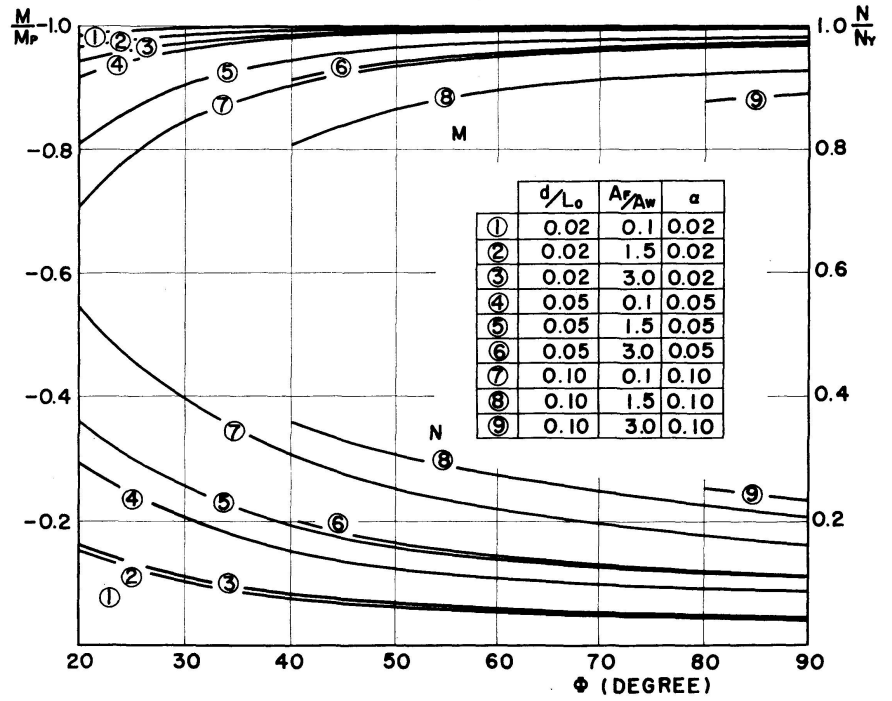

	d/L₀	Af/Aw	α
①	0.02	0.1	0.02
②	0.02	1.5	0.02
③	0.02	3.0	0.02
④	0.05	0.1	0.05
⑤	0.05	1.5	0.05
⑥	0.05	3.0	0.05
⑦	0.10	0.1	0.10
⑧	0.10	1.5	0.10
⑨	0.10	3.0	0.10

Fig. 16. Critical Bending Moment and Axial Thrust at Hinge "*b*" Under Combined Loading.

Table 3. Locations of Plastic Hinge Formation under Ultimate Load (Concentrated Loading)
(Degree)

d/L_0	A_F/A_W	ψ	ϕ								
			10°	20°	30°	40°	50°	60°	70°	80°	90°
0.02	0.1	*a*	5.81	11.68	16.92	21.50	24.88	26.55	25.80	23.21	17.23
		b	3.45	6.89	10.62	14.65	19.21	24.51	30.81	37.88	46.30
	1.5	*a*	5.71	11.52	16.88	21.50	24.88	26.49	25.80	23.21	17.23
		b	3.49	6.96	10.63	14.64	19.21	24.53	30.81	37.87	46.29
	3.0	*a*	5.52	11.52	16.88	21.50	24.88	26.49	25.80	23.21	17.14
		b	3.57	6.96	10.63	14.64	19.20	24.52	30.81	37.87	46.33
0.05	0.1	*a*	5.46	11.39	16.80	21.40	24.88	26.49	25.80	23.21	17.14
		b	3.60	7.01	10.66	14.68	19.20	24.52	30.80	37.87	46.33
	1.5	*a*	—	10.87	16.51	21.30	24.75	26.46	25.80	23.21	17.14
		b	—	7.20	10.75	14.69	19.21	24.49	30.76	37.84	46.33
	3.0	*a*	—	—	16.13	21.04	24.50	26.40	25.76	23.21	17.14
		b	—	—	10.89	14.76	19.28	24.47	30.74	37.82	46.32
0.10	0.1	*a*	5.32	10.75	16.40	21.09	24.75	26.46	25.80	23.21	17.14
		b	3.64	7.25	10.80	14.76	19.20	24.48	30.76	37.84	46.33
	1.5	*a*	—	—	15.20	20.40	24.30	26.25	25.76	23.19	17.00
		b	—	—	11.22	14.94	19.24	24.41	30.63	37.75	46.37
	3.0	*a*	—	—	—	—	—	26.08	25.80	22.69	16.91
		b	—	—	—	—	—	24.33	30.48	38.04	46.39

Table 4. Locations of Plastic Hinge Formation under Ultimate Load (Combined Loading)
(Degree)

d/L_0	α	A_F/A_W	ψ	ϕ							
				20°	30°	40°	50°	60°	70°	80°	90°
0.02	0.02	0.1	*a*	11.48	16.50	20.38	22.17	21.43	18.10	13.36	8.00
			b	7.20	11.43	16.62	22.98	30.80	39.37	48.54	57.59
		1.5	*a*	11.31	16.59	20.73	23.04	23.00	20.35	15.70	10.36
			b	7.43	11.00	15.80	21.67	28.70	36.92	45.97	54.97
		3.0	*a*	11.19	16.50	20.73	23.19	23.17	20.76	16.16	10.63
			b	7.43	11.00	15.69	21.38	28.35	36.51	45.27	54.18
0.05	0.05	0.1	*a*	11.07	16.24	20.15	21.87	21.25	17.90	13.13	8.00
			b	7.43	11.61	16.73	23.27	30.80	39.57	48.54	57.60
		1.5	*a*	10.49	15.97	20.15	22.75	22.83	20.14	15.46	9.84
			b	7.43	11.08	16.73	21.67	28.70	37.53	46.20	55.23
		3.0	*a*	—	—	19.92	22.60	23.17	20.35	15.70	10.10
			b	—	—	16.50	22.25	29.05	37.12	45.97	54.97
0.10	0.10	0.1	*a*	9.97	19.45	19.45	21.14	20.77	17.37	12.66	7.22
			b	7.96	16.97	16.97	23.47	31.38	40.19	49.00	58.12
		1.5	*a*	—	—	18.87	21.73	21.73	19.12	14.53	8.79
			b	—	—	16.62	22.98	30.10	37.94	46.90	55.76
		3.0	*a*	—	—	—	—	—	—	14.30	8.79
			b	—	—	—	—	—	—	47.37	56.02

c) Location of plastic hinges. The locations of plastic hinges at the collapse of arches due to a concentrated and combined loadings are shown in Tables 3 and 4, respectively. The locations of plastic hinges are almost constant, not so

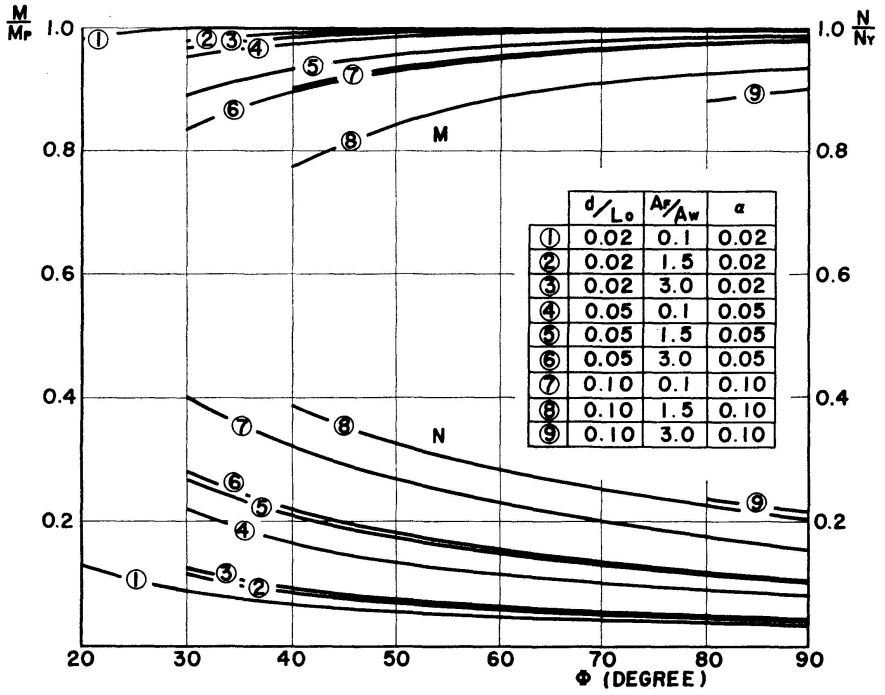

Fig. 17. Critical Bending Moment and Axial Thrust at Hinge "*a*" Under Shake-down Loading (Combined).

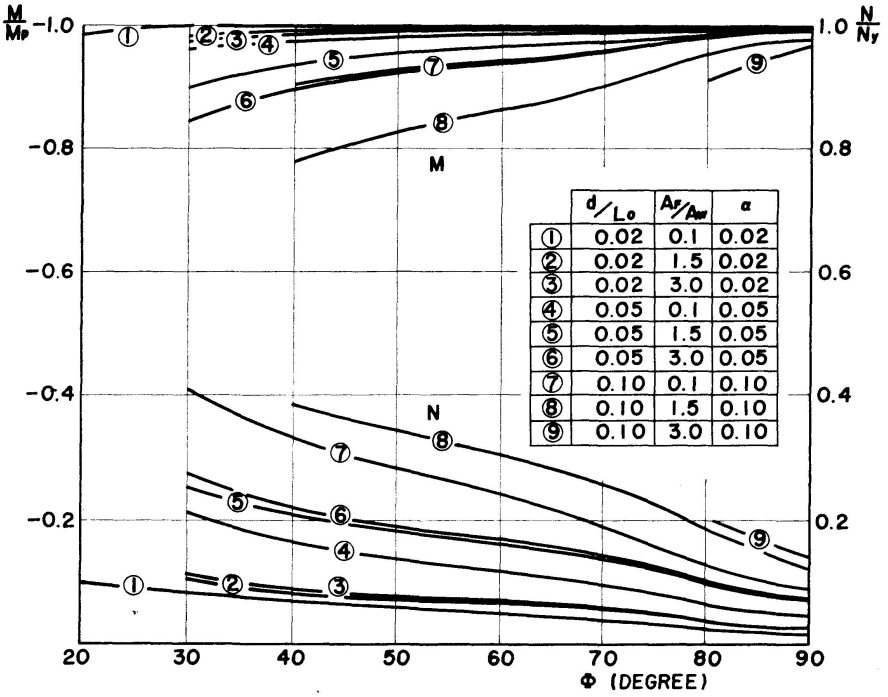

Fig. 18. Critical Bending Moment and Axial Thrust at Hinge "*b*" Under Shake-down Loading (Combined).

largely influenced by variations in d/L_0 and A_F/A_W. The difference between the locations of plastic hinges for axial thrust considered and neglected is less than a few percent of half span length L_0.

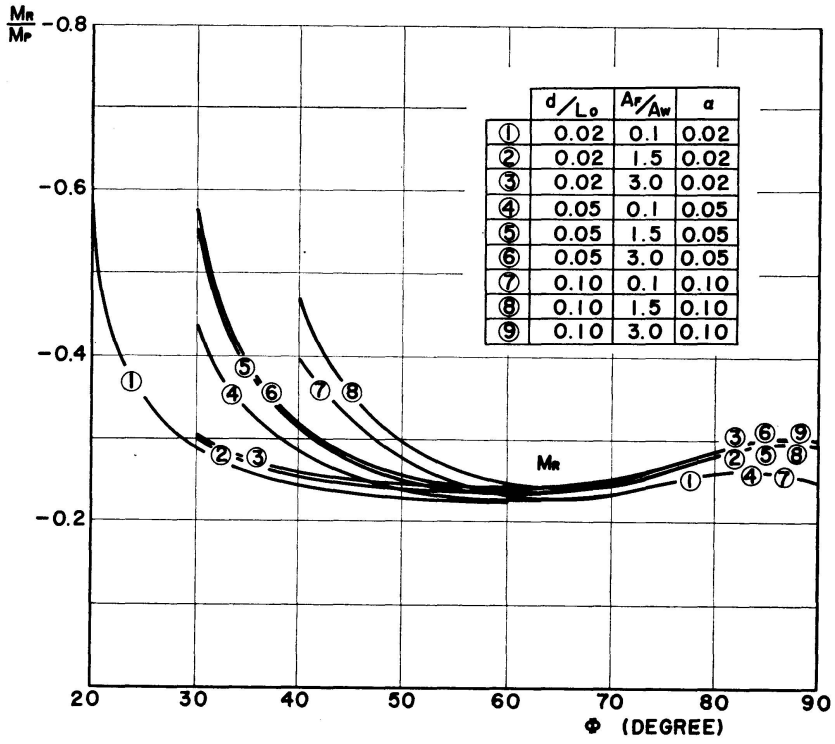

Fig. 19. Residual Moment at Hinge "a".

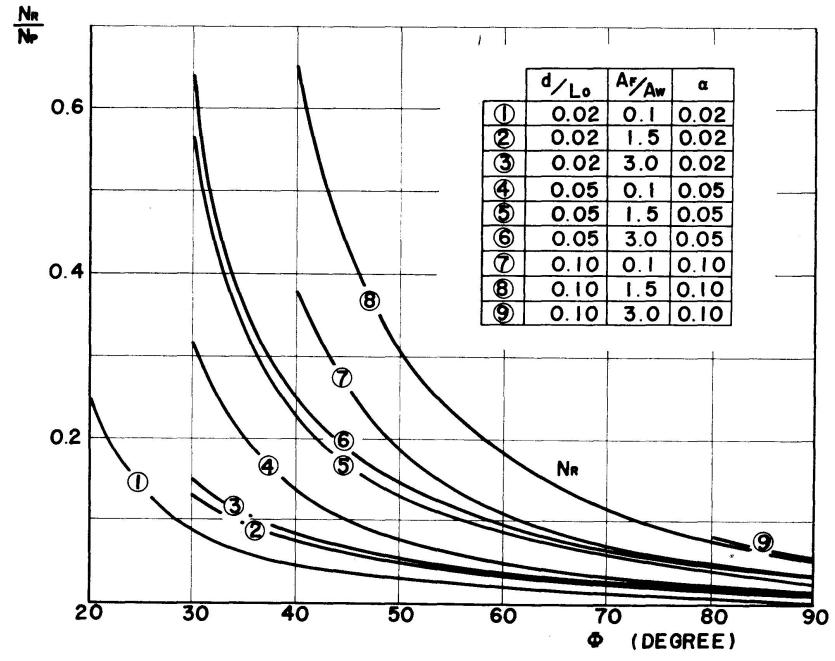

Fig. 20. Residual Thrust at Hinge "a".

2. *Shakedown Load*

a) Shakedown load. Shakedown loads due to a concentrated and combined loadings are indicated on the lower line in Tables 1 and 2 together with the ultimate load.

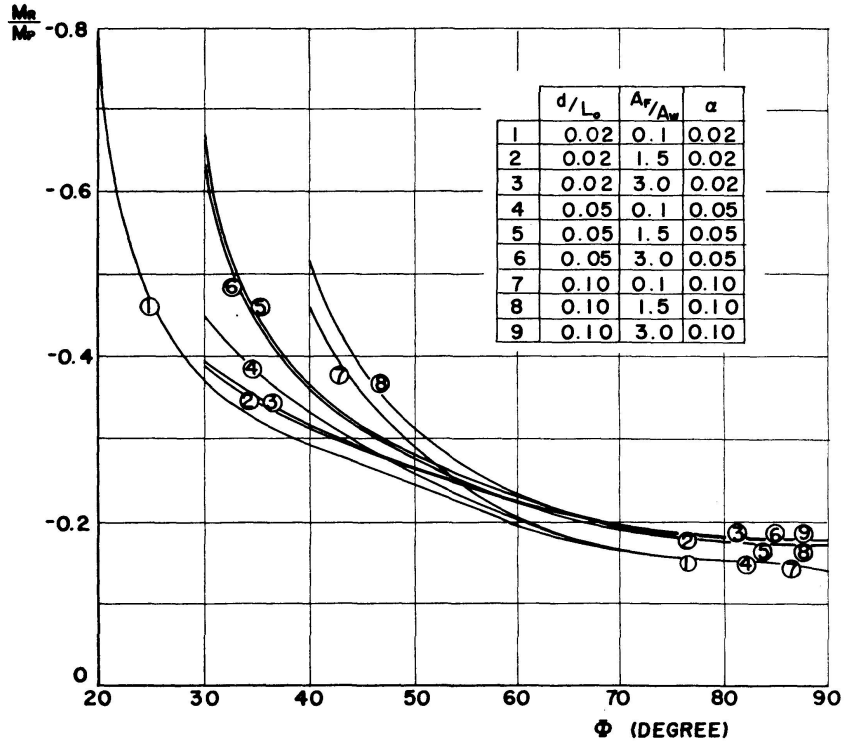

Fig. 21. Residual Moment at Hinge "*b*".

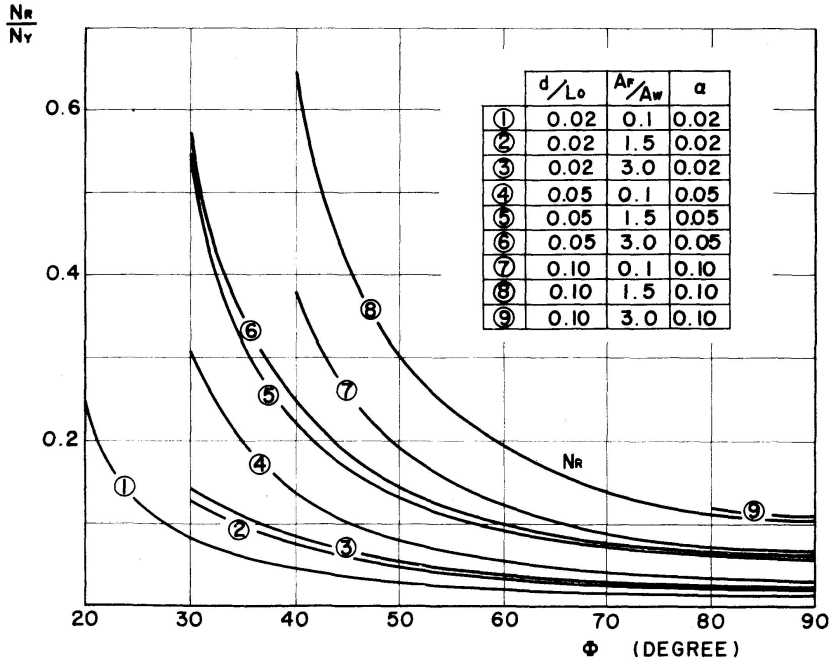

Fig. 22. Residual Thrust at Hinge "*b*".

b) Bending moments and axial thrusts at plastic hinges. The magnitudes of bending moments and axial thrusts at plastic hinges "*a*" and "*b*", when plastic hinges form under shakedown combined load, are shown in Figs. 17 and 18, respectively. These figures show the same tendency in Figs. 15 and 16.

The residual bending moment and axial thrust at plastic hinges "*a*" and "*b*" when plastic hinges form under shakedown load, are shown in Figs. 19, 20 and 21, 22, respectively. As known from these figures, the residual bending moments are almost constant at $\phi = 90°$ to 50° and rapidly increase with further reduction of ϕ. But residual axial thrust increase with reduction of ϕ from 90° to 0°.

c) Locations of plastic hinges. The locations of plastic hinges "*a*", "*b*" and loading point of a concentrated load and combined load under shakedown load are indicated in Tables 5 and 6, respectively.

In the range of used parameter, the location of plastic hinge "*a*" coincides with the loading point of a concentrated load.

Table 5. Loading Points and Locations of Plastic Hinge Formation under Shake-down Load (Concentrated Loading)

(Degree)

d/L_0	A_F/A_W		ϕ								
			10°	20°	30°	40°	50°	60°	70°	80°	90°
0.02	0.1	ψ_a	6.24	12.61	18.75	24.28	28.61	31.64	31.90	27.13	4.07
		ψ_b	3.92	7.97	12.21	16.59	21.39	26.82	32.48	38.88	45.54
		θ_b	4.08	8.03	11.64	15.00	17.45	19.72	20.92	20.71	18.75
	1.5	ψ_a	6.24	12.61	18.75	24.08	28.61	31.64	31.90	27.13	5.32
		ψ_b	4.24	8.10	12.36	16.79	21.39	26.82	32.48	38.88	45.54
		θ_b	3.76	7.65	11.40	14.69	17.65	19.72	20.92	20.46	18.75
	3.0	ψ_a	6.16	12.61	18.60	24.08	28.61	31.64	31.90	27.29	6.20
		ψ_b	4.16	8.10	12.36	16.79	21.39	26.82	32.48	38.88	45.54
		θ_b	3.52	7.65	11.40	14.69	17.65	19.72	20.70	20.50	18.57
0.05	0.1	ψ_a	6.16	12.61	18.60	24.08	28.61	31.64	31.90	27.29	6.20
		ψ_b	4.16	8.10	12.36	16.79	21.39	26.82	32.48	38.88	45.54
		θ_b	3.52	7.65	11.40	14.69	17.65	19.72	20.77	20.50	18.57
	1.5	ψ_a	5.22	12.14	18.36	24.03	28.61	31.64	32.12	27.50	9.08
		ψ_b	4.50	8.40	12.36	16.79	21.65	26.82	32.48	38.88	45.82
		θ_b	2.90	7.12	11.06	14.44	17.39	19.56	20.52	20.25	18.29
	3.0	ψ_a	—	—	18.06	23.72	28.61	31.64	32.26	27.91	11.07
		ψ_b	—	—	12.75	17.00	21.65	26.82	32.62	38.88	45.93
		θ_b	—	—	10.44	14.03	17.01	19.26	20.38	20.25	18.18
0.10	0.1	ψ_a	4.82	11.81	18.21	23.82	28.56	31.66	32.12	27.50	9.54
		ψ_b	4.50	8.45	12.60	16.79	21.60	26.76	32.48	38.88	45.82
		θ_b	3.06	7.17	11.02	14.44	17.34	19.50	20.52	20.25	18.29
	1.5	ψ_a	—	10.38	17.24	23.19	28.35	31.64	32.62	28.86	14.71
		ψ_b	—	9.09	12.99	17.32	21.78	27.13	32.62	39.03	46.11
		θ_b	—	5.74	9.82	13.40	16.37	18.45	19.81	19.59	17.53
	3.0	ψ_a	—	—	—	22.68	27.97	31.80	33.28	30.31	18.18
		ψ_b	—	—	—	17.68	22.35	27.13	32.92	39.29	46.52
		θ_b	—	—	—	12.20	15.25	17.68	18.82	18.72	16.55

Table 6. Loading Points and Locations of Plastic Hinge Formation (Combined Loading)

(Degree)

d/L_0	α	A_F/A_W		ϕ							
				20°	30°	40°	50°	60°	70°	80°	90°
0.02	0.02	0.1	ψ_a	12.15	18.40	23.40	26.69	26.47	16.63	0.05	0.02
			ψ_b	7.93	12.89	18.23	24.40	31.52	39.37	47.66	56.62
			θ_b	9.24	11.53	14.42	16.73	18.08	18.29	17.00	13.59
		1.5	ψ_a	—	18.32	23.62	27.48	28.60	23.95	0.52	0.06
			ψ_b	—	12.64	17.78	23.54	30.00	37.42	45.30	53.81
			θ_b	—	11.68	14.52	16.98	18.63	18.94	17.91	14.79
		3.0	ψ_a	—	18.32	23.62	27.48	28.95	25.00	1.52	0.13
			ψ_b	—	12.73	17.67	23.40	29.83	37.04	44.90	53.13
			θ_b	—	11.59	14.52	16.98	18.63	19.08	18.08	15.09
0.05	0.05	0.1	ψ_a	—	17.79	23.15	26.60	26.50	16.84	0.35	0.13
			ψ_b	—	12.81	18.37	24.56	31.57	39.49	47.70	56.81
			θ_b	—	12.20	14.40	16.55	17.93	18.06	16.91	13.25
		1.5	ψ_a	—	17.10	23.15	27.19	28.60	24.18	2.91	0.39
			ψ_b	—	12.55	18.02	23.69	30.35	37.65	45.60	54.18
			θ_b	—	12.73	14.29	16.55	18.10	18.47	17.38	14.30
		3.0	ψ_a	—	16.66	22.92	27.33	28.95	25.41	6.88	0.66
			ψ_b	—	12.81	18.13	23.83	30.17	37.45	45.36	53.66
			θ_b	—	12.29	13.81	16.10	17.76	18.27	17.14	14.30
0.10	0.10	0.1	ψ_a	—	15.78	22.45	26.17	26.33	17.04	1.05	0.39
			ψ_b	—	12.11	18.60	25.00	32.10	39.90	48.16	57.07
			θ_b	—	15.00	14.40	16.11	17.41	17.45	16.21	12.73
		1.5	ψ_a	—	—	21.52	26.60	28.60	25.20	8.51	1.44
			ψ_b	—	—	18.72	24.71	31.22	38.67	46.76	55.23
			θ_b	—	—	13.70	15.09	16.53	16.84	15.74	12.46
		3.0	ψ_a	—	—	—	—	—	—	14.11	2.76
			ψ_b	—	—	—	—	—	—	47.00	55.50
			θ_b	—	—	—	—	—	—	14.34	11.15

3. Alternating Plasticity Load

The numerical results of laternating plasticity load are indicated in Table 7. The critical cross sections and the loading points are indicated by upper line and lower line in Table 8, respectively.

Table 7. Alternative Plasticity Load

(N_y)

d/L_0	A_F/A_W	ϕ								
		10°	20°	30°	40°	50°	60°	70°	80°	90°
0.02	0.1	0.0256	0.0258	0.0259	0.0259	0.0260	0.0260	0.0261	0.0262	0.0264
	1.5	0.0499	0.0505	0.0508	0.0510	0.0511	0.0511	0.0512	0.0514	0.0517
	3.0	0.0570	0.0578	0.0582	0.0584	0.0585	0.0585	0.0586	0.0588	0.0592
0.05	0.1	0.0636	0.0642	0.0645	0.0648	0.0648	0.0649	0.0650	0.0652	0.0656
	1.5	0.1227	0.1250	0.1264	0.1275	0.1274	0.1271	0.1272	0.1275	0.1282
	3.0	0.1397	0.1426	0.1446	0.1459	0.1457	0.1454	0.1454	0.1457	0.1464
0.10	0.1	0.1280	0.1278	0.1288	0.1297	0.1295	0.1292	0.1293	0.1296	0.1302
	1.5	0.2020	0.2480	0.2517	0.2551	0.2535	0.2521	0.2515	0.2515	0.2524
	3.0	0.2173	0.2826	0.2875	0.2919	0.2896	0.2879	0.2869	0.2868	0.2876

Table 8. Alternative Plasticity Load (Locations of Load)
(Degree)

d/L_0	A_F/A_W	ψ	ϕ								
			10°	20°	30°	40°	50°	60°	70°	80°	90°
0.02	0.1	*a*	5.66	11.08	16.34	21.19	25.48	29.29	32.17	33.88	33.86
		b	3.34	6.82	10.15	13.30	16.62	19.12	21.25	23.10	24.95
	1.5	*a*	5.73	11.19	16.40	21.25	25.45	29.27	32.17	33.93	33.87
		b	3.15	6.63	9.94	13.08	16.85	19.30	21.45	23.26	25.14
	3.0	*a*	5.79	11.21	16.40	21.30	25.42	29.27	32.17	33.93	33.91
		b	3.10	6.59	9.88	13.02	16.94	19.39	21.53	23.36	25.17
0.05	0.1	*a*	5.73	11.21	16.40	21.30	25.39	29.23	32.19	33.92	33.91
		b	3.15	6.59	9.91	12.99	17.01	19.49	21.59	23.41	25.25
	1.5	*a*	5.91	11.42	16.61	21.46	25.27	29.17	32.16	33.94	34.04
		b	2.94	6.18	9.40	12.49	17.62	20.07	22.14	23.93	25.68
	3.0	*a*	5.99	11.50	16.67	21.49	25.21	29.12	32.15	34.00	34.07
		b	2.81	6.06	9.29	12.37	17.83	20.25	22.31	24.08	25.82
0.10	0.1	*a*	5.80	11.36	16.56	21.43	25.21	29.10	32.15	33.94	34.00
		b	3.21	6.32	9.54	12.58	17.74	20.19	22.21	23.99	25.75
	1.5	*a*	1.65	11.70	16.89	21.66	24.85	28.92	32.09	34.01	34.24
		b	9.90	5.75	8.81	11.78	19.25	21.50	23.47	25.12	26.68
	3.0	*a*	8.51	11.77	16.98	21.77	24.78	28.87	32.06	34.05	34.31
		b	9.90	5.60	8.60	11.52	19.70	21.94	23.86	25.41	26.96

4. Comparison of the Three Loads

The shakedown load is always less than the ultimate load but it is not less than 96% of the ultimate load in the range considered.

The ratio of shakedown load and ultimate load is minimum at $\phi = 30°$ to $50°$ and for a concentrated load only is maximum at $\phi = 90°$.

The ultimate load and the shakedown load for a concentrated load and the combined load are shown in Figs. 23 and 24, respectively. The alternating plasticity loads are also shown by chained lines in these figures.

From these figures, it is found that the alternative plasticity load is almost less than the corresponding shakedown load and the difference between the two loads becomes obvious against the uniformly distributed load coefficient α.

Conclusions

This paper presents the theroretical analysis of the minimum static collapse load, shakedown load and alternative plasticity load of two-hinged circular steel arches under a concentrated load, uniformly distributed load and their combined load. The corresponding loads are calculated using center angle of arches, span length, cross sectional properties as parameters. Cross sectional shapes of arch ribs are rectangular, box or I section with double symmetric axes.

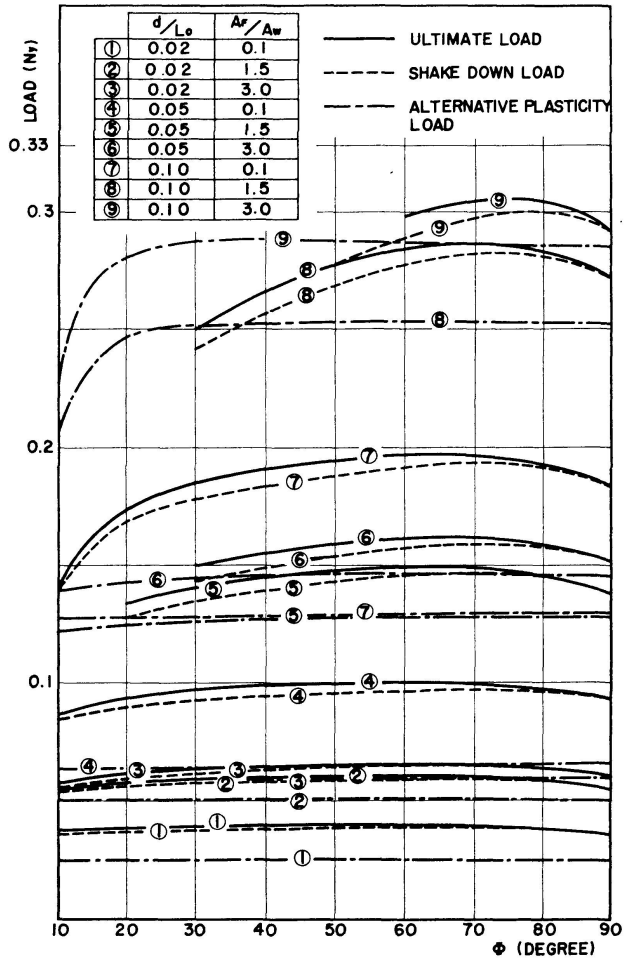

Fig. 23.

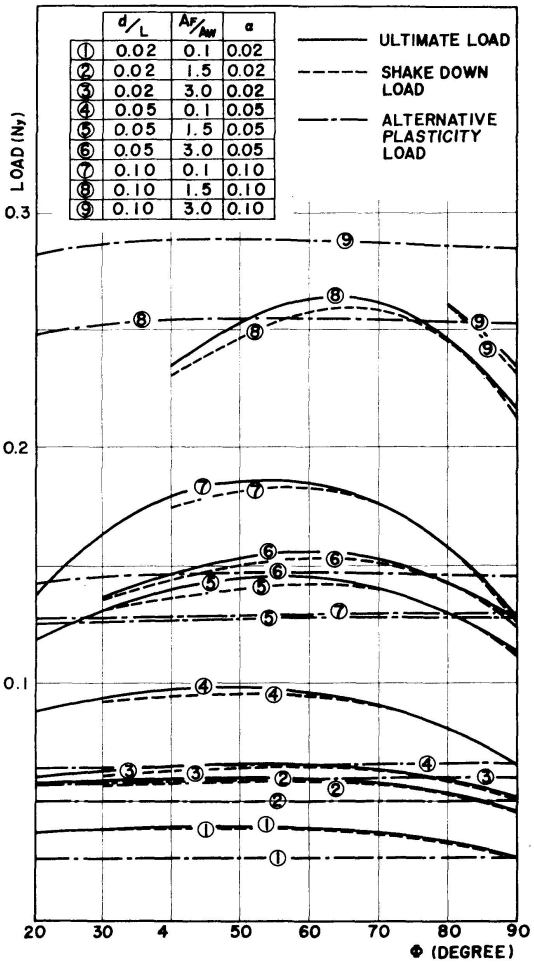

Fig. 24.

Main conclusions obtained from the results of this study are as follows.

1. The ultimate load and shakedown load are compared numerically in Tables 1 and 2. The difference between the loads is about 5% at the most and can be neglected.

2. The plastic hinges "*a*" and "*b*" due to ultimate load are located nearer the center of the span than the plastic hinges "*a*" and "*b*" due to shakedown load.

3. The alternating bending moment due to variable repeated load yield a section "*a*" (Table 8) and the arches collapse due to alternating plasticity yielding at the cross section by alternating bending moment. This alternating plasticity loads are less than the shakedown load for the range of given arch properties and the differences of both loads are shown in Figs. 23 and 24. Both loads for the combined load considered uniformly distributed dead load become nearly equal but the consideration for both ultimate and alternative loads may be required for the plastic analysis of arches.

References

1. ONAT, E. T. and PRAGER, W.: Limit Analysis of Arches, Jour. of Mech. and Physics of Solids, Vol. 1, No. 2, Jan. 1953.
2. YOKOO, Y. and YAMAGATA, K.: A Study on the Final States of Arches (the case carrying a concentrated load) (in Japanese), Trans. of Architectural Institute of Japan, No. 58, Feb., 1958.
   —: A Study on the Final States of Arches (the case carrying uniformly distributed load) (in Japanese), Trans. of AIJ, No. 59, June, 1958.
3. YAMASAKI, T. and ISHIKAWA, N.: Elasto-Plastic Analysis of Circular Arches (in Japanese), Trans. of Japan Society of Civil Engineers, No. 158, Oct., 1968.
4. EYRE, D. G. and GALAMBOS, T. V.: Variable Repeated Loading – A Literature, Research Report No. 3, Structures Division, Washington University, Sept. 1967.
5. FRANCIOSI, V., AUGUSTI, G. and SPARACIO, R.: Collapse of Arches under Repeated Loading, Proc. of ASCE, Vol. 90, ST 1, Feb. 1964.

Summary

The theoretical analysis of shakedown load of structures applying a bending moment and an axial thrust is described and the loads are calculated for two hinged steel circular arches with I, box or rectangular cross sections. The calculated results for concentrated, uniformly distributed and their combined loadings are compared for the minimum static collapse load, shakedown load and alternative plasticity load.

Résumé

On présente une analyse théorique de structures soumises à une charge de stabilisation (shakedown load) et entraînant un moment de flexion et un effort axial. Les charges sont calculées pour des arcs circulaires en acier à deux articulations et de section rectangulaire, en caisson ou en I. Les résultats trouvés pour des charges concentrées, uniformément réparties ou leurs combinaisons sont comparées pour la charge de rupture statique minimale, pour la charge de stabilisation (shakedown load) et pour la charge de plasticité alternative.

Zusammenfassung

Die theoretische Berechnung der "shake-down"-Last von Tragwerken mit Biegemoment und Horizontalschub wird vorgelegt und für einen stählernen Zweigelenk-Kreisbogen mit T-, Kasten- oder Rechteckquerschnitt berechnet. Die Ergebnisse für konzentrierte, gleichförmig verteilte und kombinierte Belastung werden mit jenen für die minimale statische Trag-, "shake-down"- und die entsprechende plastische Last verglichen.